Cureus Journal of Computer Science
https://doi.org/10.7759/s44389-026-00038-6

Original Article

Machine Learning–Based Prediction and Interpretability Analysis of Aircraft Engine Landing and Take-Off Emissions

Somashekar V [1], Shivakumar PN [1]

1. *Department of Aeronautical Engineering, Nitte Meenakshi Institute of Technology (NMIT) Nitte (Deemed to be University), Bangalore, IND*

Received: February 08, 2026 | Review began: February 17, 2026 | Review ended: March 02, 2026 | Published: March 10, 2026

© **Copyright** 2026
This is an open access article distributed under the terms of the Creative Commons Attribution License CC-BY 4.0., which permits unrestricted use, distribution, and reproduction in any medium, provided the original author and source are credited.

Abstract

This study presents a comprehensive data-driven framework for predicting aircraft engine emissions under Landing and Take-Off (LTO) conditions using certified data from the ICAO (The International Civil Aviation Organization) Aircraft Engine Emissions Databank. The primary objective is to develop reliable machine learning (ML) models for estimating emission indices of nitrogen oxides (NOx), carbon monoxide (CO), and unburned hydrocarbons (HC), while simultaneously providing physical interpretability of model behaviour. The methodology involves systematic data preprocessing, feature selection, and the application of multiple ML algorithms, including Random Forest, Gradient Boosting, Support Vector Machine, Artificial Neural Network, and Linear Regression models. Model performance was evaluated using statistical metrics and Taylor diagram analysis, while interpretability was assessed through feature importance, partial dependence plots, individual conditional expectation plots, and error variability analysis across thrust classes and LTO phases. Quantitative results show that ensemble models outperform other approaches, with the Random Forest model achieving correlation coefficients of approximately 0.95 for NOx, 0.80 for CO, and 0.70 for HC, along with superior variance representation. Fuel flow emerged as the most influential parameter, contributing nearly 80% for NOx, over 60% for CO, and approximately 45% for HC, while thrust and pressure ratio exhibited pollutant-specific secondary influences. Error variability analysis revealed higher uncertainty for CO and HC during idle and low-thrust regimes, whereas NOx prediction uncertainty was dominated by climb-out and take-off phases. The study concludes that data-driven ensemble ML models, combined with interpretability analysis, provide a robust and physically consistent approach for aircraft engine emissions prediction, offering valuable insights for emission mitigation strategies and regulatory assessment.

Categories: AI applications, IoT Applications, Machine Learning (ML)

Keywords: machine learning, aircraft engine emissions, icao lto cycle, model interpretability, emission index prediction

Introduction

Aircraft engine emissions remain a critical environmental concern due to their direct contribution to local air quality degradation around airports and their indirect impact on global climate change. Pollutants such as nitrogen oxides (NOx), carbon monoxide (CO), and unburned hydrocarbons (HC) generated during aircraft engine operation play a significant role in ozone formation, secondary particulate matter, and atmospheric chemical imbalance. As a result, international aviation regulatory bodies have established stringent certification and monitoring frameworks to quantify and control these emissions, particularly during the landing and take-off (LTO) cycle, which dominates ground-level pollutant exposure.

The aviation industry remains a critical pillar of global connectivity, yet its rapid growth poses significant challenges to environmental sustainability and public health [1-6]. Aircraft engines emit a complex array of pollutants during the LTO cycle, including NOx, CO, and ultrafine particles, which are known precursors to respiratory and cardiovascular issues in near-airport communities [7-8]. While road traffic has historically dominated urban air quality research, recent studies suggest that airport-related emissions can contribute up to 24% of local ambient NO_2 under normal conditions [9-13].

Quantifying these emissions is inherently difficult due to the dynamic nature of aircraft movement and the nonlinear interaction between engine thrust, fuel composition, and meteorology. Traditional dispersion models often assume linear additivity and fail to capture episodic high-impact events driven by specific runway operations. To address these complexities, machine learning (ML) algorithms have emerged as robust alternatives, capable of learning patterns from high-dimensional datasets without requiring detailed physical models [14-20]. Specifically, tree-based ensemble methods like XGBoost have demonstrated high predictive accuracy in modeling pollutant concentrations.

However, the "black-box" nature of advanced ML models presents a barrier to their implementation in mission-critical aviation contexts [21-25]. There is a pressing need for model interpretability to ensure that predictions align with established atmospheric physics and provide actionable insights for stakeholders [26]. Recent advancements in explainable AI, such as the use of SHapley Additive Explanations, allow researchers to fairly attribute the variance in air quality to specific features like wind direction, planetary boundary layer height, and arrival/departure frequencies.

Motivated by these challenges, the present study develops a comprehensive data-driven framework for predicting aircraft engine LTO emissions using certified ICAO databank information. Multiple ML models are evaluated and systematically compared using advanced statistical and visualization techniques. Beyond prediction accuracy, the study emphasizes interpretability through feature importance analysis, partial dependence plots, individual conditional expectation analysis, error variability assessment across thrust classes and LTO phases, and low-dimensional data visualization. By combining predictive performance with physical interpretability, this work aims to bridge the gap between data-driven modeling and regulatory-relevant emission analysis.

The contributions of this study are threefold: (i) development and comparison of multiple ML models for predicting NOx, CO, and HC emission indices using certified LTO data; (ii) quantitative assessment of model performance and uncertainty across operating regimes; and (iii) comprehensive interpretability analysis linking ML predictions to underlying combustion and operational characteristics. The findings provide valuable insights for emission assessment, mitigation strategy development, and future regulatory-oriented modeling of aircraft engine emissions.

Materials And Methods

Figure *1* presents the structured workflow adopted in this study for the analysis and prediction of aircraft engine emissions under the ICAO LTO cycle framework. The workflow visually summarizes the sequential stages of the research methodology, beginning with certified data acquisition and culminating in model evaluation and interpretability analysis. The diagram is designed to emphasize methodological transparency, reproducibility, and regulatory alignment.

The workflow begins with the certified emissions data source, namely the ICAO Aircraft Engine Emissions Databank, accessed through the European Union Aviation Safety Agency environmental portal. This databank provides standardized engine-level emissions measurements obtained under controlled certification conditions. The inclusion of this stage highlights that the study relies exclusively on regulatory-approved and globally recognized emissions data, ensuring consistency and comparability across engine types.

The second stage represents the selection of engine operating parameters, which constitute the primary predictive inputs. Key variables extracted from the databank include fuel flow, thrust, and pressure ratio. These parameters were chosen due to their direct physical relevance to combustion processes and pollutant formation mechanisms. The diagram illustrates that emission behaviour is analyzed as a function of measurable thermodynamic and operational characteristics rather than abstract features.

The central component of the workflow corresponds to the ML modeling framework. Multiple supervised learning algorithms - including Random Forest, Gradient Boosting, Artificial Neural Networks (ANN), Support Vector Machines (SVM), and Linear Regression - were implemented to capture both linear and non-linear relationships between engine

parameters and emission indices. The training and validation sub-stage indicates the systematic partitioning of the dataset and model calibration procedures used to ensure generalization and robustness.

Following model development, the workflow proceeds to the model interpretation and evaluation stage, which forms a critical contribution of the study. This stage integrates feature importance analysis, partial dependence plots (PDP), individual conditional expectation (ICE) plots, error variability assessment, and Taylor diagram evaluation. The inclusion of these techniques highlights that the study not only evaluates predictive accuracy but also investigates the physical consistency and sensitivity of model behaviour across operating regimes.

The dataset was divided into training and testing subsets using a fixed random split to ensure consistent evaluation across models. Default hyperparameters were applied to all algorithms to maintain fairness in comparative assessment and to focus the analysis on relative model behavior and interpretability rather than extensive parameter optimization.

The final stage of the workflow illustrates the emission prediction outputs, specifically the estimation of NOx, CO, and HC emission indices. By positioning these outputs after interpretability and validation steps, the diagram underscores that predictions are supported by statistical reliability and mechanistic plausibility. The graphical abstract structure therefore conveys a closed analytical loop linking certified data, computational modeling, physical interpretation, and quantitative validation.

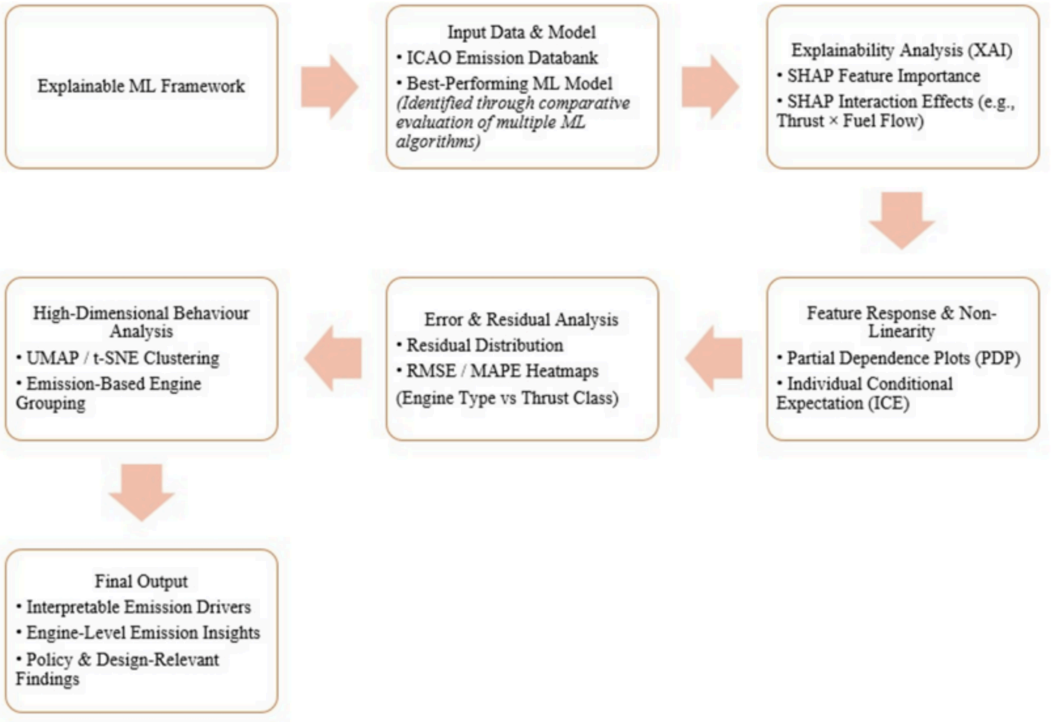


FIGURE 1: ICAO LTO Cycle–Based Aircraft Engine Emissions Analysis Workflow

ICAO, International Civil Aviation Organization; LTO, Landing and Take-Off; MAPE, Mean Absolute Percentage Error; ML, Machine Learning; RMSE, Root Mean Squared Error; SHAP, SHapley Additive Explanations; t-SNE. t-distributed Stochastic Neighbor Embedding; UMAP, Uniform Manifold Approximation and Projection

Results And Discussion

Explainability and feature influence

Figure 2 illustrates the relative importance of input parameters influencing the prediction of carbon monoxide emission index (CO EI). Fuel flow emerges as the dominant parameter, contributing approximately 63-65% of the total feature importance, indicating that CO formation is strongly governed by combustion completeness and fuel supply rate. Thrust accounts for about 20-22%, reflecting its secondary influence through operating regime changes associated with engine power settings. Pressure ratio shows the least contribution at roughly 14-15%, suggesting a comparatively weaker impact on CO emissions under the analyzed conditions. The dominance of fuel flow highlights that CO emissions are primarily driven by fuel-air mixing and combustion efficiency, particularly under low-temperature or incomplete combustion regimes typical of certain LTO modes.

The feature importance distribution for hydrocarbon emission index (HC EI) reveals a more distributed influence among the input variables, as shown in Figure 3. Fuel flow remains the most influential parameter, contributing approximately 43-45%, confirming its central role in unburned HC formation. Pressure ratio and thrust exhibit comparable contributions, accounting for nearly 27-29% each. This balanced influence indicates that HC emissions are sensitive not only to fuel supply but also to combustion pressure conditions and engine operating thrust. The result signifies that HC emissions are affected by both thermodynamic efficiency and flow residence time, especially under low-power operating modes where incomplete combustion is more prevalent.

The feature importance results for nitrogen oxides emission index (NOx EI) demonstrate a strong dominance of fuel flow, contributing approximately 78-80% of the total importance, as shown in Figure 4. This indicates that NOx formation is highly sensitive to fuel-dependent combustion temperature and heat release characteristics. Thrust shows a moderate influence of around 13-14%, reflecting its indirect effect on combustion temperature through engine power settings. Pressure ratio contributes minimally, at approximately 6-8%, suggesting that within the examined operational range, its role in NOx formation is secondary. The results confirm that NOx emissions are primarily governed by high-temperature combustion processes associated with increased fuel flow during higher thrust conditions.

Across all three pollutants, fuel flow consistently dominates feature importance, contributing more than 40% in HC EI, over 60% in CO EI, and nearly 80% in NOx EI, establishing it as the most critical parameter for emission prediction. Thrust and pressure ratio play pollutant-specific secondary roles, with HC emissions showing the strongest sensitivity to combined engine operating parameters. These findings provide quantitative evidence supporting the physical linkage between fuel supply, combustion characteristics, and regulated aircraft engine emissions.

Non-linear behaviour

Figure 5 partial dependence plots for CO EI show distinct non-linear sensitivities to thrust, fuel flow, and pressure ratio. CO EI initially increases with thrust, reaching a pronounced peak at intermediate thrust levels, before stabilizing at higher thrust. This behaviour reflects incomplete combustion at low- and mid-power settings, where lower flame temperatures and reduced oxidation rates promote CO formation, while improved combustion efficiency at higher thrust limits further increases. In contrast, CO EI exhibits a sharp decrease with increasing fuel flow, indicating that higher fuel flow regimes - typically associated with higher combustion temperatures - enhance CO oxidation to CO_2. The pressure ratio shows a monotonic decreasing trend, suggesting that improved compression and enhanced air-fuel mixing at higher pressure ratios significantly suppress CO emissions. Overall, the PDPs confirm that CO emissions reminder strongly associated with low-temperature combustion regimes typical of idle and approach phases.

The PDPs for HC EI reveal strong sensitivity to all three parameters, with thrust exhibiting a pronounced peak at intermediate values, as shown in Figure 6. This indicates that HC emissions are highest when combustion is incomplete due to suboptimal residence time and flame stability. At higher thrust levels, HC EI decreases and stabilizes, implying improved fuel burnout. Fuel flow shows a steep declining trend, demonstrating that increasing fuel flow enhances combustion completeness and reduces unburned HC. Similarly, HC EI decreases steadily with increasing pressure ratio, highlighting the role of higher compression in improving fuel atomization and oxidation. These trends collectively indicate that HC emissions are most critical under low-power operating conditions and are significantly mitigated at higher combustion efficiency regimes.

The NOx EI partial dependence plots exhibit behaviour distinctly different from CO and HC as shown in Figure *7*. Fuel flow shows a strong monotonic increase, indicating that NOx formation is highly sensitive to increased combustion temperatures driven by higher fuel flow. Pressure ratio also exhibits a consistent increasing trend, reflecting enhanced thermal NOx formation under high-pressure, high-temperature conditions. Thrust shows a more complex, non-linear response, with localized peaks and troughs, suggesting that thrust alone does not directly govern NOx formation but influences it indirectly through coupled thermodynamic effects. These results confirm that NOx emissions are dominated by high-temperature combustion processes, particularly during climb-out and take-off phases.

The PDP analysis provides clear, physically consistent insights into pollutant formation mechanisms. CO and HC emissions are predominantly associated with low-temperature, incomplete combustion regimes, while NOx emissions are governed by high-temperature thermodynamic conditions. Fuel flow emerges as the most influential parameter across all pollutants, but with opposite trends for incomplete combustion products (CO, HC) and thermal NOx formation. The results demonstrate the capability of PDP analysis to capture non-linear emission behaviour and reinforce the importance of operating-condition-specific mitigation strategies for aircraft engine emissions.

The Figure *8* ICE plots for CO EI reveal substantial heterogeneity in the response of individual engines to variations in thrust and fuel flow. In the thrust-based ICE plot, individual curves show a wide spread at low and intermediate thrust levels, indicating that CO emissions respond differently across engines under partial power conditions. The average trend demonstrates a gradual increase in CO EI with thrust, followed by a plateau at higher thrust levels, suggesting improved combustion stability and oxidation efficiency at elevated power settings. The dispersion among individual curves highlights engine-specific combustion characteristics and operational variability during low-power regimes.

In contrast, the fuel-flow-based ICE plot exhibits a strong and consistent decreasing trend in CO EI as fuel flow increases. Most individual curves converge rapidly at higher fuel flow values, indicating reduced inter-engine variability under high fuel flow conditions. This behaviour confirms that higher fuel flow rates promote higher combustion temperatures and more complete oxidation of CO-to-CO_2. The reduced spread at higher fuel flow signifies a dominant and uniform physical mechanism governing CO formation across engines.

The ICE analysis confirms that CO emissions are highly sensitive to fuel flow with low variability at higher operating regimes, while thrust effects remain engine-dependent, particularly at low and mid-thrust conditions typical of idle and approach phases.

The Figure *9* thrust-based ICE plot for HC EI shows pronounced non-linear behaviour with substantial spread among individual engine responses. HC emissions increase sharply at intermediate thrust levels for several engines, indicating incomplete combustion and poor fuel oxidation under transitional power conditions. At higher thrust levels, the average curve stabilizes, and variability reduces, reflecting improved combustion efficiency and reduced unburned HCs.

The fuel-flow ICE plot demonstrates a steep decline in HC EI with increasing fuel flow, with most individual curves rapidly collapsing toward low emission levels. This convergence suggests that HC emissions are strongly governed by fuel flow, and once sufficient fuel flow is achieved, combustion completeness becomes dominant across all engines. Minor residual variability at low fuel flow indicates sensitivity to engine design and atomization efficiency.

These results highlight that HC emissions exhibit strong engine-to-engine variability at low thrust and low fuel flow but become largely uniform at higher fuel flow rates, emphasizing the importance of controlling low-power operating conditions for HC mitigation.

The Figure *10* thrust-based ICE plot for NOx EI shows a generally decreasing average trend with increasing thrust, accompanied by moderate dispersion among individual curves. This indicates that thrust alone does not directly control NOx formation and that other coupled thermodynamic parameters influence NOx behaviour. The variability suggests different engine responses to thrust changes, particularly in mid-thrust regimes.

In contrast, the fuel-flow ICE plot exhibits a strong, monotonic increase in NOx EI with increasing fuel flow, with most individual curves following a similar upward trend. The relatively narrow spread at higher fuel flow levels indicates a consistent thermal NOx formation mechanism across engines. This behaviour reflects the strong dependence of NOx formation on combustion temperature, which rises with increased fuel flow.

The ICE plots clearly demonstrate that NOx emissions are predominantly fuel-flow driven, with limited dependence on thrust alone. The consistent upward trends confirm that high-temperature combustion regimes dominate NOx formation across different engine types.

Engine-level insights

The heatmap illustrates the variability in prediction error for the CO EI across different thrust categories and LTO phases. The highest error variability is consistently observed during the idle phase, particularly for very low (VL) and medium (M) thrust categories, with peak values exceeding 20. This indicates that CO emissions are most difficult to predict under idle conditions, where incomplete combustion, flame instability, and engine-specific control strategies introduce significant dispersion. In contrast, take-off and climb-out phases show minimal error variability across all thrust categories, reflecting more stable combustion conditions and stronger coupling between fuel flow and CO oxidation. The relatively lower variability at high (H) thrust further suggests improved model reliability at higher power settings.

Significance

Figure *11* demonstrates that CO emission prediction uncertainty is dominated by low-power operating regimes, emphasizing the need for refined modeling or phase-specific correction strategies during idle and approach conditions.

The HC EI error variability heatmap exhibits a pattern similar to CO but with overall lower magnitudes, as shown in Figure *12*. The idle phase again shows the highest variability, particularly for VL thrust engines, where error values reach nearly 16. This behaviour reflects the strong sensitivity of HC emissions to combustion completeness and fuel atomization quality at low power. Variability decreases significantly with increasing thrust category, and take-off and climb-out phases consistently exhibit minimal error across all thrust classes. The high (H) and very high (VH) thrust categories show particularly low variability, indicating stable and predictable HC emission behaviour.

Significance

The results confirm that HC emission prediction is most challenging during low-thrust idle operation, while higher thrust regimes yield robust and reliable model performance. This highlights the importance of low-power regime characterization in HC emissions modeling.

Unlike CO and HC, the NOx error variability heatmap shows its highest values during the climb-out and take-off phases, especially for low (L), medium (M), and high (H) thrust categories, with peak variability reaching approximately 12. In contrast, the idle phase exhibits the lowest variability across all thrust categories, with values generally below 1. This trend reflects the strong dependence of NOx formation on high-temperature combustion conditions, where small variations in temperature, pressure, and residence time can lead to significant differences in NOx production. The relatively higher variability at high-power phases indicates increased sensitivity of NOx predictions to operational and engine-specific parameters.

Figure *13* highlights that NOx emission prediction uncertainty is dominated by high-power operating modes, underscoring the complexity of modeling thermal NOx formation during climb-out and take-off conditions.

The error variability analysis reveals that incomplete combustion products (CO and HC) exhibit maximum prediction uncertainty during idle and low-thrust regimes, whereas NOx emissions show greater uncertainty during high-power phases. These trends are physically consistent with known combustion mechanisms and confirm that model performance is phase-dependent. The results provide critical insight into where predictive models are most reliable and where targeted refinement is required, strengthening the credibility and interpretability of the overall emissions analysis.

Figure *14* t-SNE plot presents a two-dimensional embedding of the high-dimensional aircraft engine emissions dataset, where each point represents an individual engine operating condition and the colour scale corresponds to NOx EI. Distinct clusters are clearly observed, indicating the presence of structured groupings in the data rather than random dispersion. These clusters reflect underlying similarities in engine operating parameters such as fuel flow, thrust, and pressure ratio, which jointly influence emission behaviour.

A clear separation between low and high NOx EI regions is evident from the colour gradient across clusters. Clusters characterized by darker colours correspond to lower NOx emission levels, typically associated with low-temperature combustion regimes, while clusters with brighter colours indicate higher NOx EI values linked to elevated combustion

temperatures and higher power operating modes. The gradual colour transitions within certain clusters suggest smooth variations in operating conditions, whereas sharp transitions between clusters indicate regime changes in combustion behaviour.

The spatial isolation of several compact clusters highlights the heterogeneity among engine classes and LTO operating modes. In particular, tightly grouped regions with relatively uniform NOx EI imply consistent emission behaviour under specific operating conditions, while elongated or dispersed clusters indicate increased sensitivity of NOx formation to small variations in engine parameters. This visualization confirms that the emissions dataset exhibits non-linear and multi-regime characteristics, which justifies the use of advanced data-driven and machine-learning-based analytical approaches.

The t-SNE visualization demonstrates that aircraft engine emissions data naturally cluster according to underlying operational and thermodynamic regimes. The clear segregation of NOx emission levels across clusters validates the physical consistency of the dataset and supports the effectiveness of the selected features in capturing emission behaviour. This analysis provides qualitative confirmation that the model inputs contain sufficient discriminatory information for reliable emissions prediction and interpretation.

The Taylor diagram summarizes the statistical performance of different ML models in predicting the CO EI by jointly representing the correlation coefficient, normalized standard deviation, and centered root-mean-square error relative to the reference observations. The Random Forest and Gradient Boosting models are positioned closest to the reference point, indicating high correlation (≈0.8) and a standard deviation comparable to the observed CO EI variability. This reflects their strong capability to capture the non-linear combustion behaviour governing CO formation. The ANN-MLP model shows moderate correlation with a slightly underestimated variance, suggesting reasonable predictive performance but reduced ability to reproduce the full spread of CO emissions. In contrast, the SVM and Linear Regression models are located farther from the reference, exhibiting low correlation and significant variance mismatch, highlighting their limitations in modeling incomplete combustion phenomena associated with CO emissions.

Figure *15* demonstrates that ensemble-based models outperform linear and kernel-based approaches for CO EI prediction, emphasizing the importance of non-linear learning mechanisms in capturing low-power combustion variability.

For HC EI prediction, the Taylor diagram reveals a broader spread among model performances, as shown in Figure *16*. The Random Forest model again exhibits the highest correlation (≈0.7) with relatively good variance matching, indicating its robustness in capturing unburned HC formation. Gradient Boosting shows slightly reduced correlation but still maintains acceptable variance representation. The ANN-MLP model demonstrates moderate correlation but noticeably underestimates variability, suggesting limited generalization across different operating regimes. SVM and Linear Regression models display very low correlation and poor variance reproduction, confirming their inadequacy for modeling HC emissions, which are highly sensitive to transient and low-thrust operating conditions.

The results highlight the complexity of HC emission behaviour and confirm that advanced ensemble learning techniques are required to accurately model the strong non-linearities present in HC emissions data.

The Taylor diagram for NOx EI shows significantly improved performance across all models compared to CO and HC. The Random Forest model is closest to the reference, with very high correlation (≈0.95) and excellent variance agreement, indicating its strong capability to capture thermal NOx formation mechanisms. Gradient Boosting and ANN-MLP models also demonstrate high correlation (≈0.88-0.92), reflecting consistent predictive skill under high-temperature combustion regimes. Even SVM and Linear Regression models perform comparatively better for NOx EI, owing to the more monotonic and physically driven relationship between NOx formation and operating parameters such as fuel flow and pressure ratio.

Figure *17* indicates that NOx emissions are inherently easier to model due to their strong thermodynamic dependence, and it validates the reliability of ML approaches - particularly ensemble methods - for NOx emission prediction.

The Taylor diagram analysis provides a comprehensive and intuitive comparison of model performance across different emission species. Ensemble models consistently demonstrate superior correlation and variance representation for all pollutants, with the most pronounced advantages observed for CO and HC emissions. The results confirm that pollutant-

specific emission mechanisms strongly influence model performance and underline the necessity of selecting appropriate ML architectures for reliable aircraft engine emissions prediction.

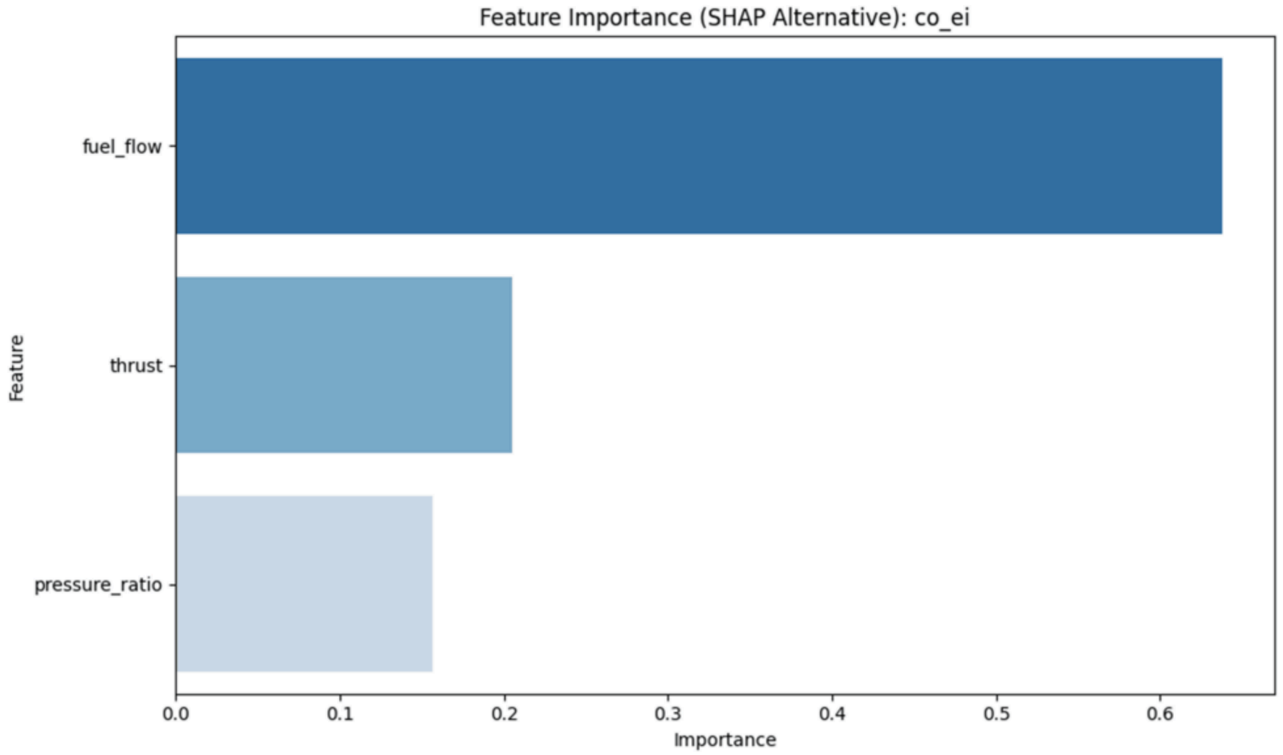


FIGURE 2: Feature Importance Analysis for CO Emission Index (CO EI)

CO, Carbon Monoxide; SHAP, SHapley Additive Explanations

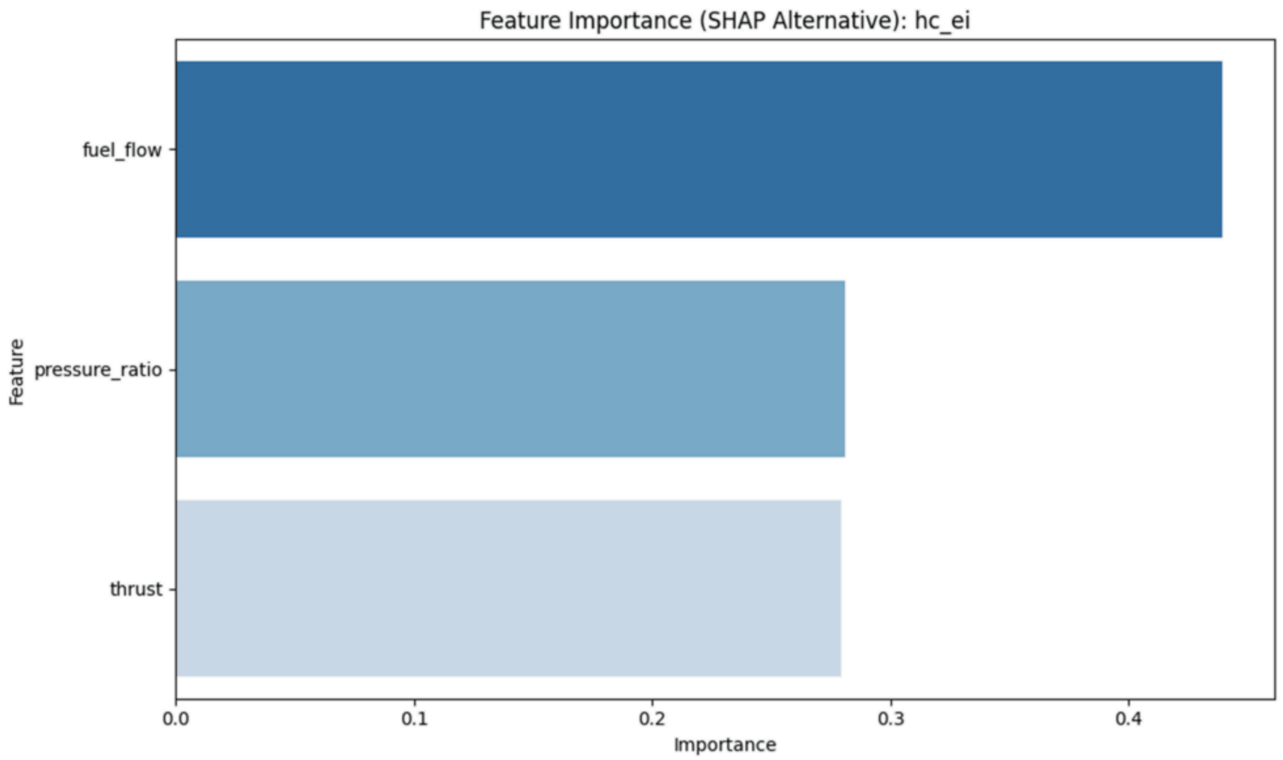


FIGURE 3: Feature Importance Analysis for HC Emission Index (HC EI)

HC, Hydrocarbons; SHAP, SHapley Additive Explanations

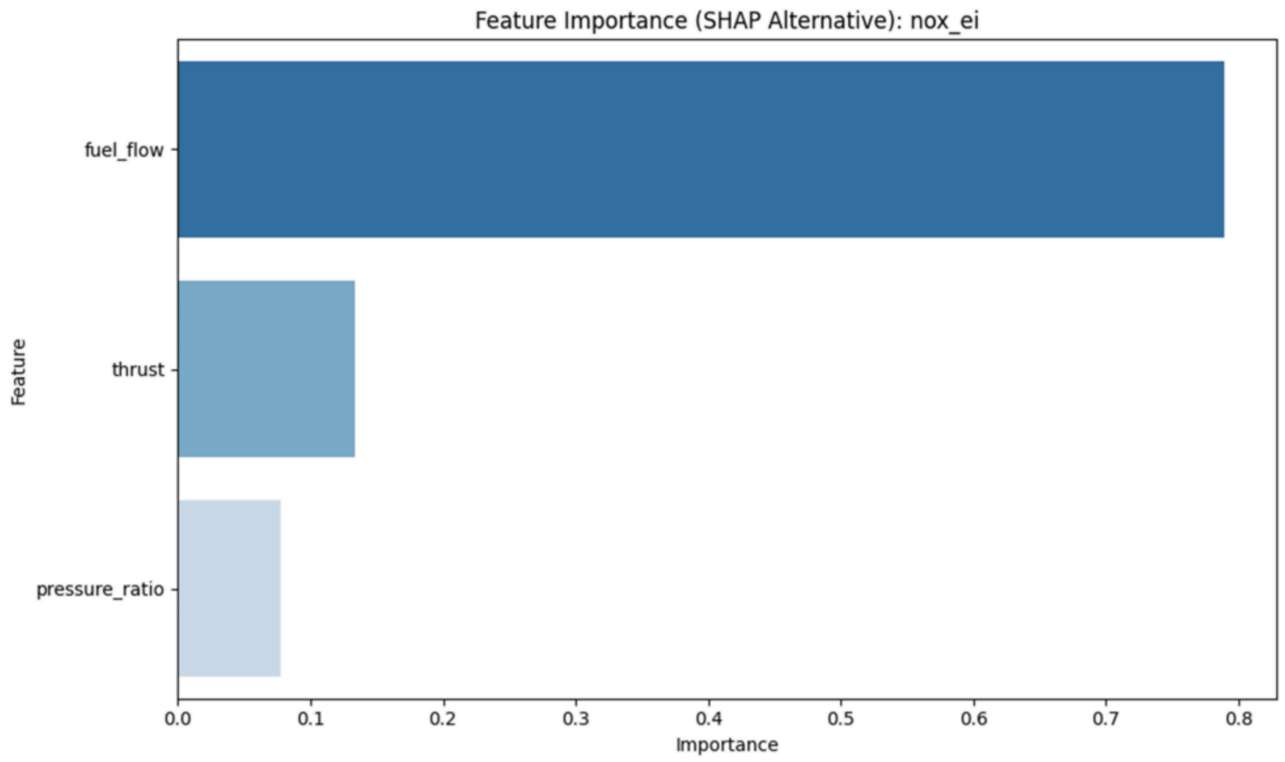


FIGURE 4: Feature Importance Analysis for NOx Emission Index (NOx EI)

SHAP, SHapley Additive Explanations

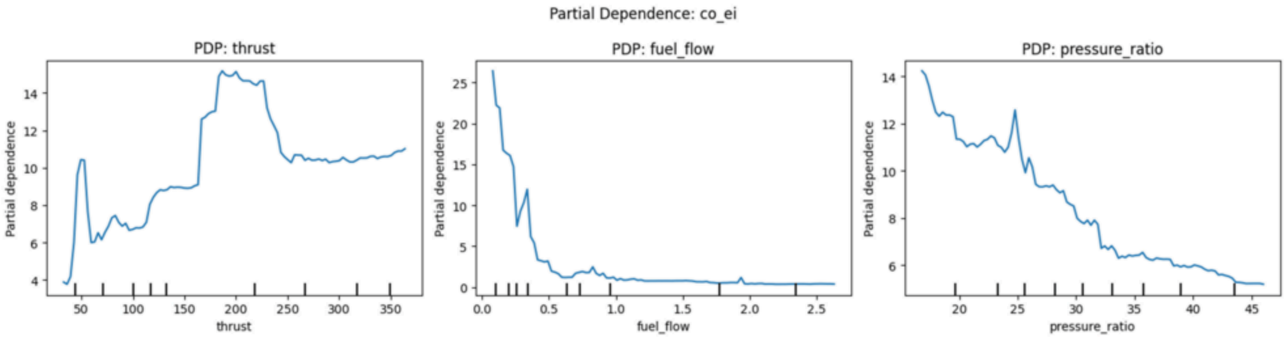


FIGURE 5: Partial Dependence Plots (PDP) of Engine Parameters on CO Emission Index (CO EI)

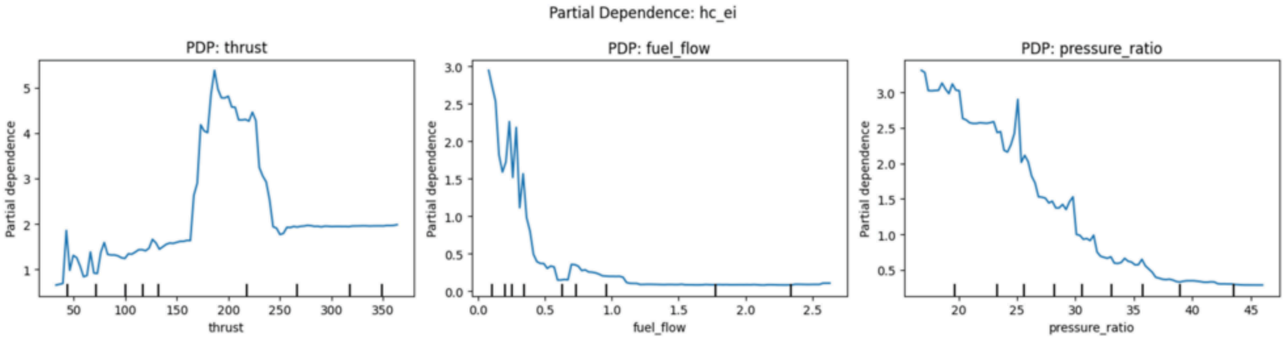


FIGURE 6: Partial Dependence Plots (PDP) of Engine Parameters on HC Emission Index (HC EI)

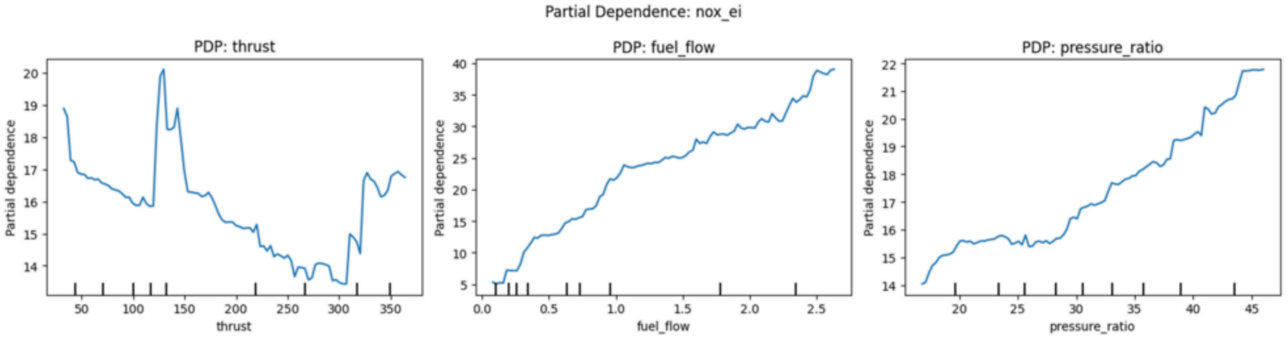


FIGURE 7: Partial Dependence Plots (PDP) of Engine Parameters on NOx Emission Index (NOx EI)

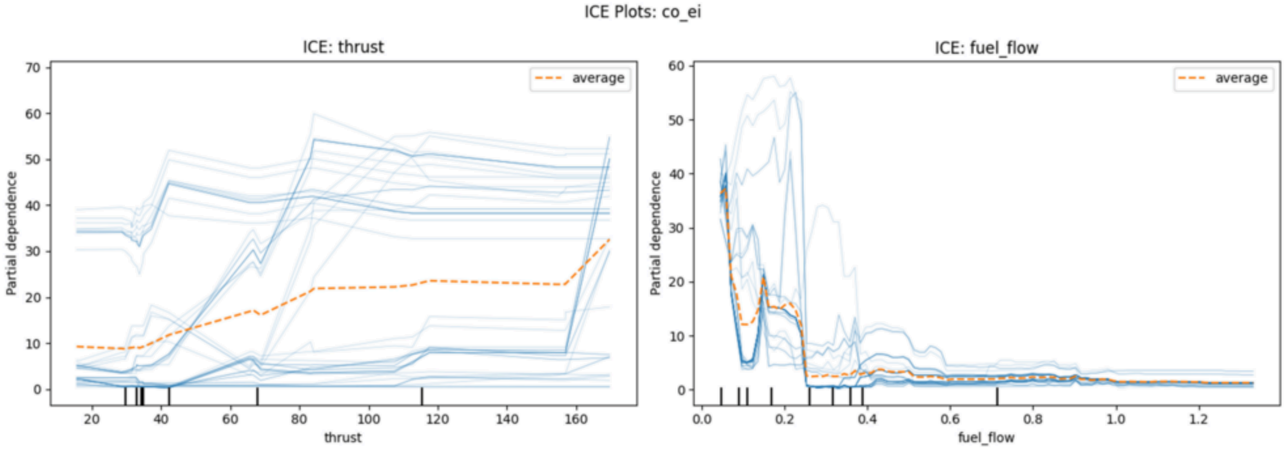


FIGURE 8: ICE Analysis of Thrust and Fuel Flow Effects on CO Emission Index (CO EI)

ICE, Individual Conditional Expectation

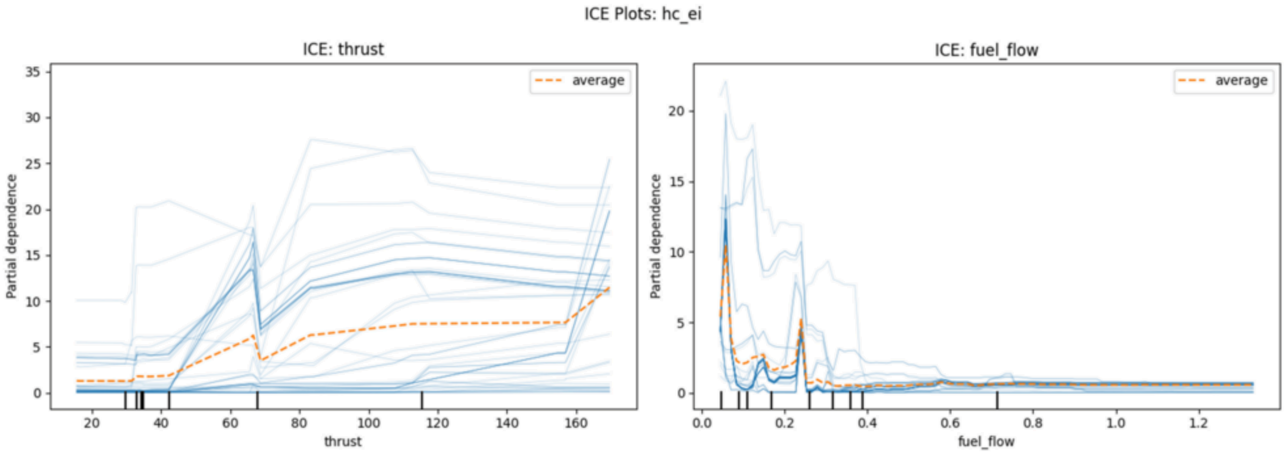


FIGURE 9: ICE Analysis of Thrust and Fuel Flow Effects on HC Emission Index (HC EI)

ICE, Individual Conditional Expectation

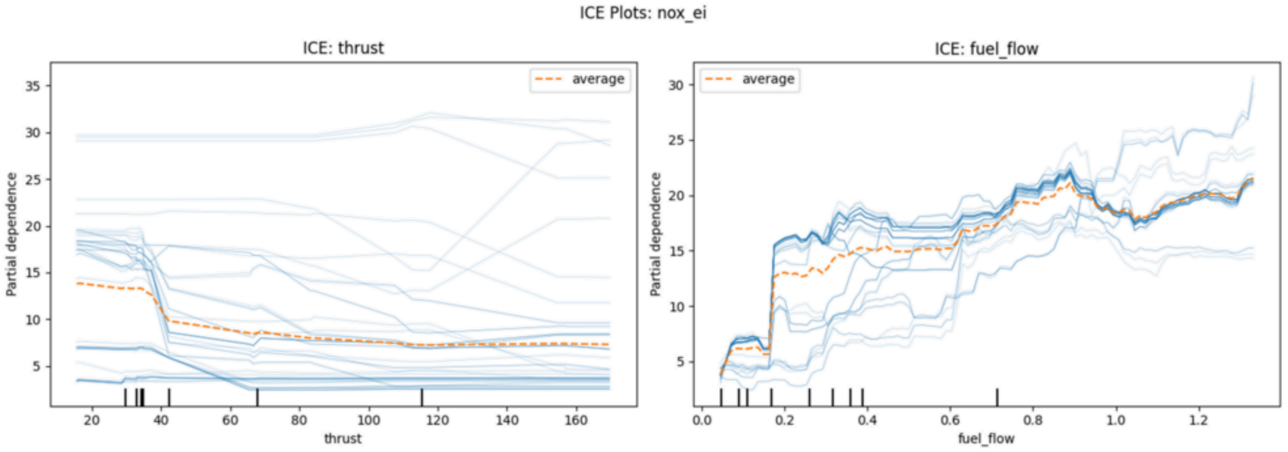


FIGURE 10: ICE Analysis of Thrust and Fuel Flow Effects on NOx Emission Index (NOx EI)

ICE, Individual Conditional Expectation

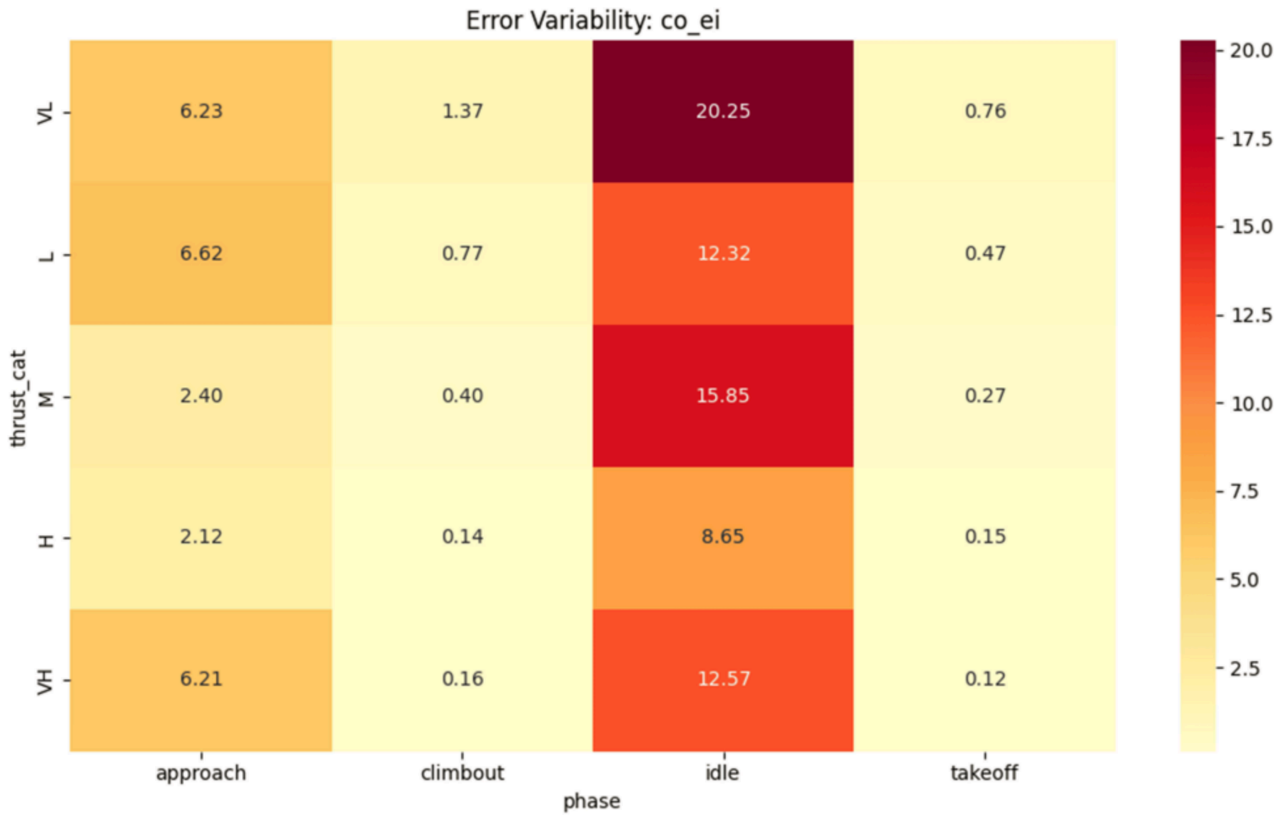


FIGURE 11: Error Variability of CO Emission Index Across Thrust Classes and LTO Phases

CO, Carbon Monoxide; LTO, Landing and Take-Off



FIGURE 12: Error Variability of HC Emission Index Across Thrust Classes and LTO Phases

HC, Hydrocarbons; LTO, Landing and Take-Off

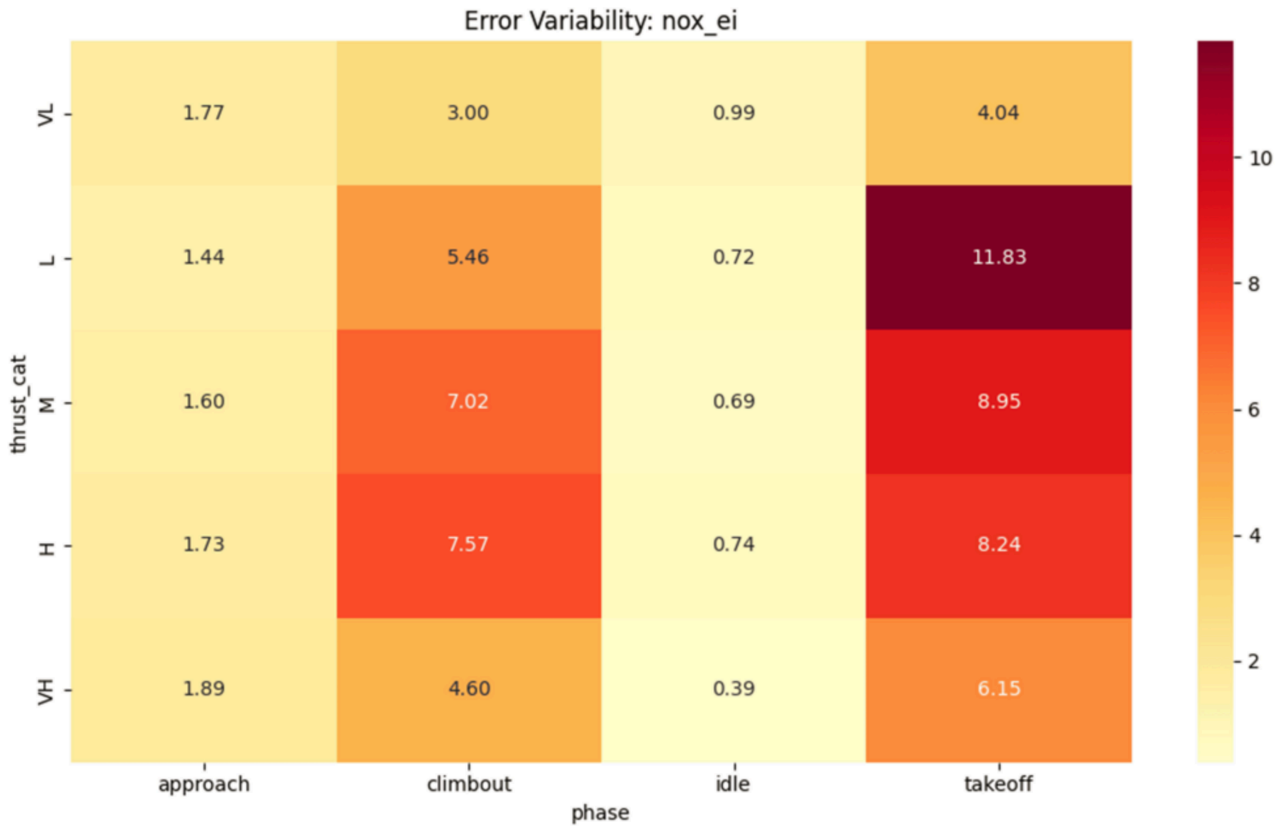


FIGURE 13: Error Variability of NOx Emission Index Across Thrust Classes and LTO Phases

LTO, Landing and Take-Off

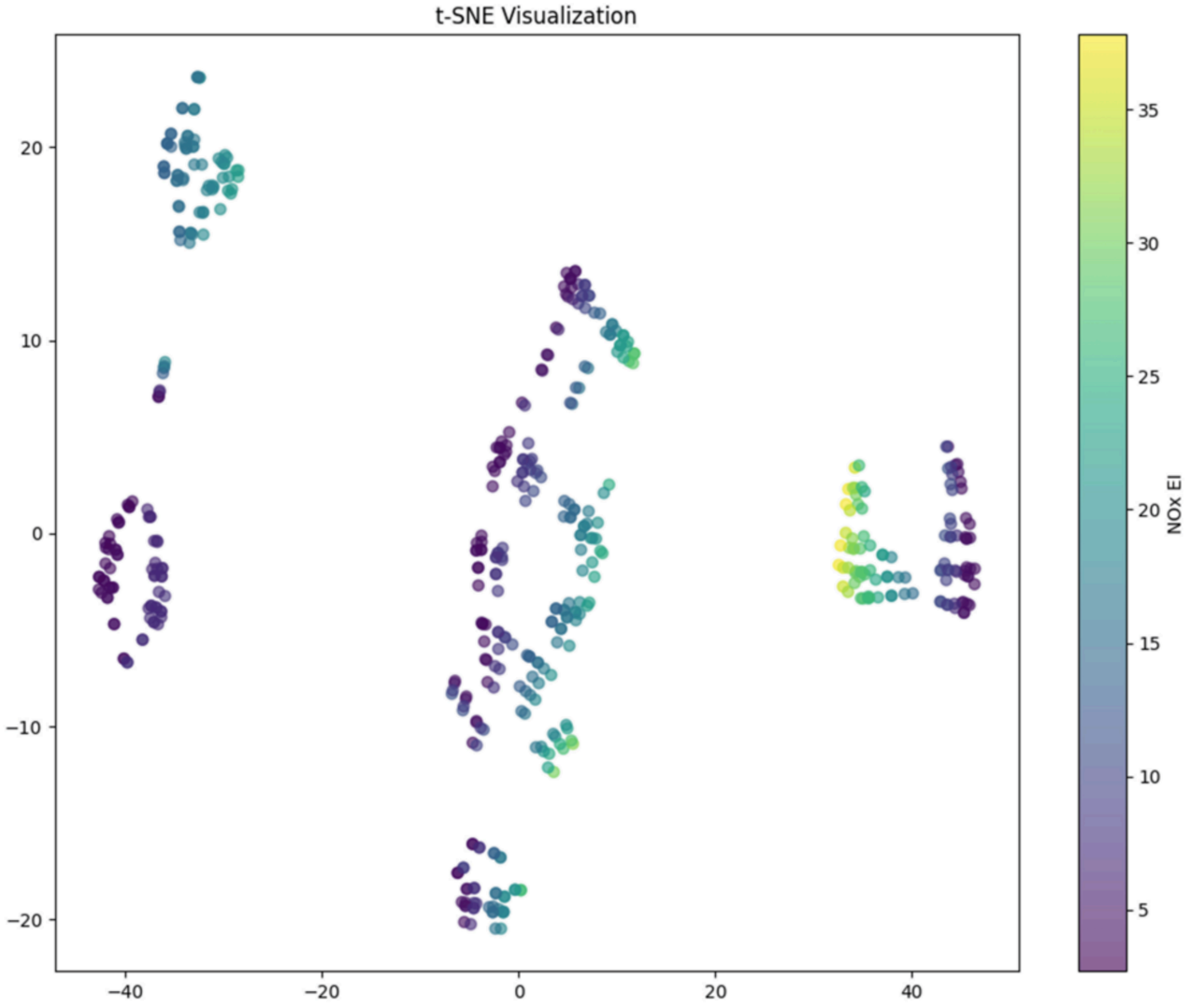


FIGURE 14: t-SNE Visualization of Aircraft Engine Emissions Data Colored by NOx Emission Index

t-SNE; T-distributed Stochastic Neighbor Embedding

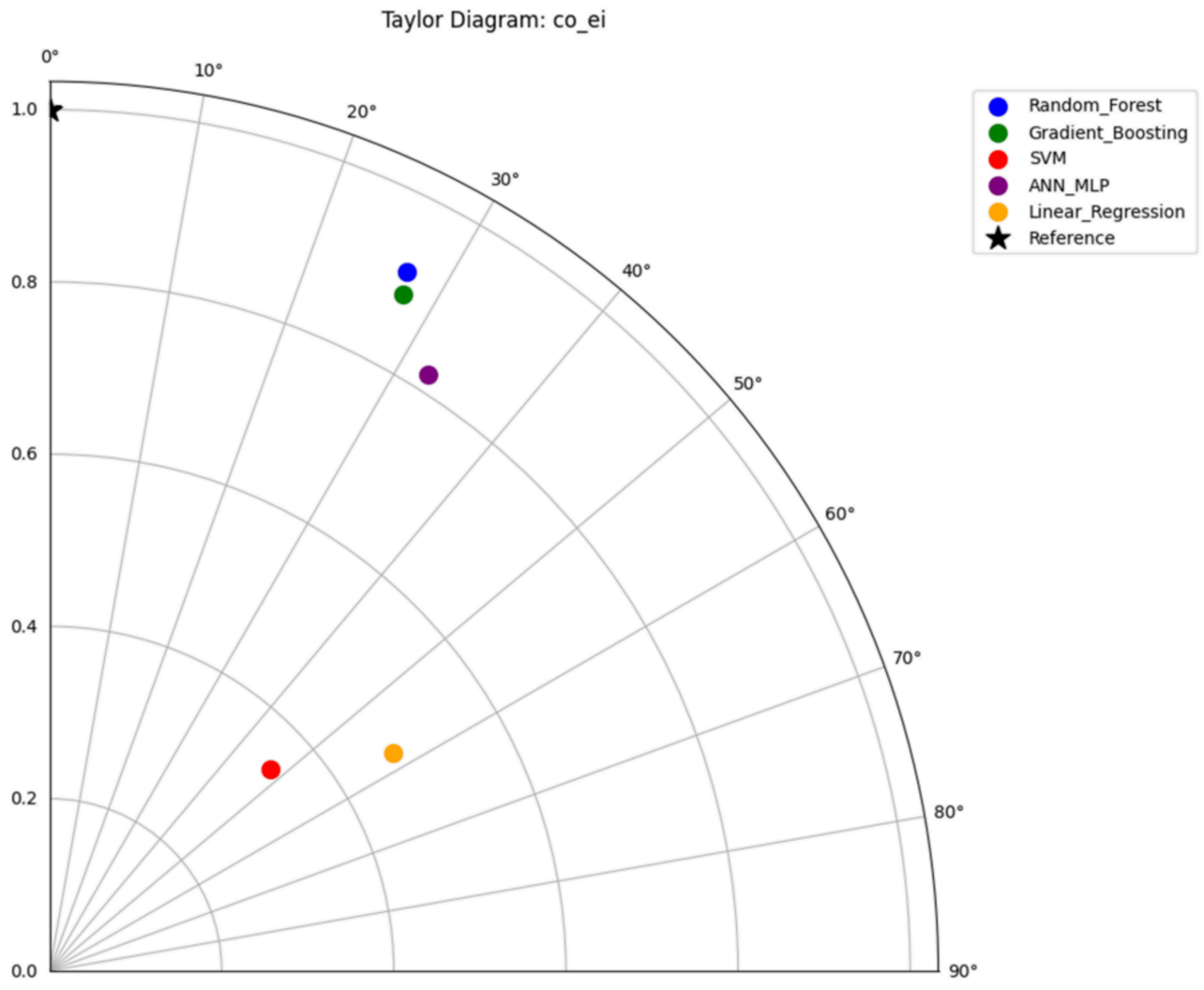


FIGURE 15: Taylor Diagram for CO Emission Index Prediction

CO, Carbon Monoxide; ANN-MLP, Artificial Neural Network-Multi-Layer Perceptron; SVM, Support Vector Machine

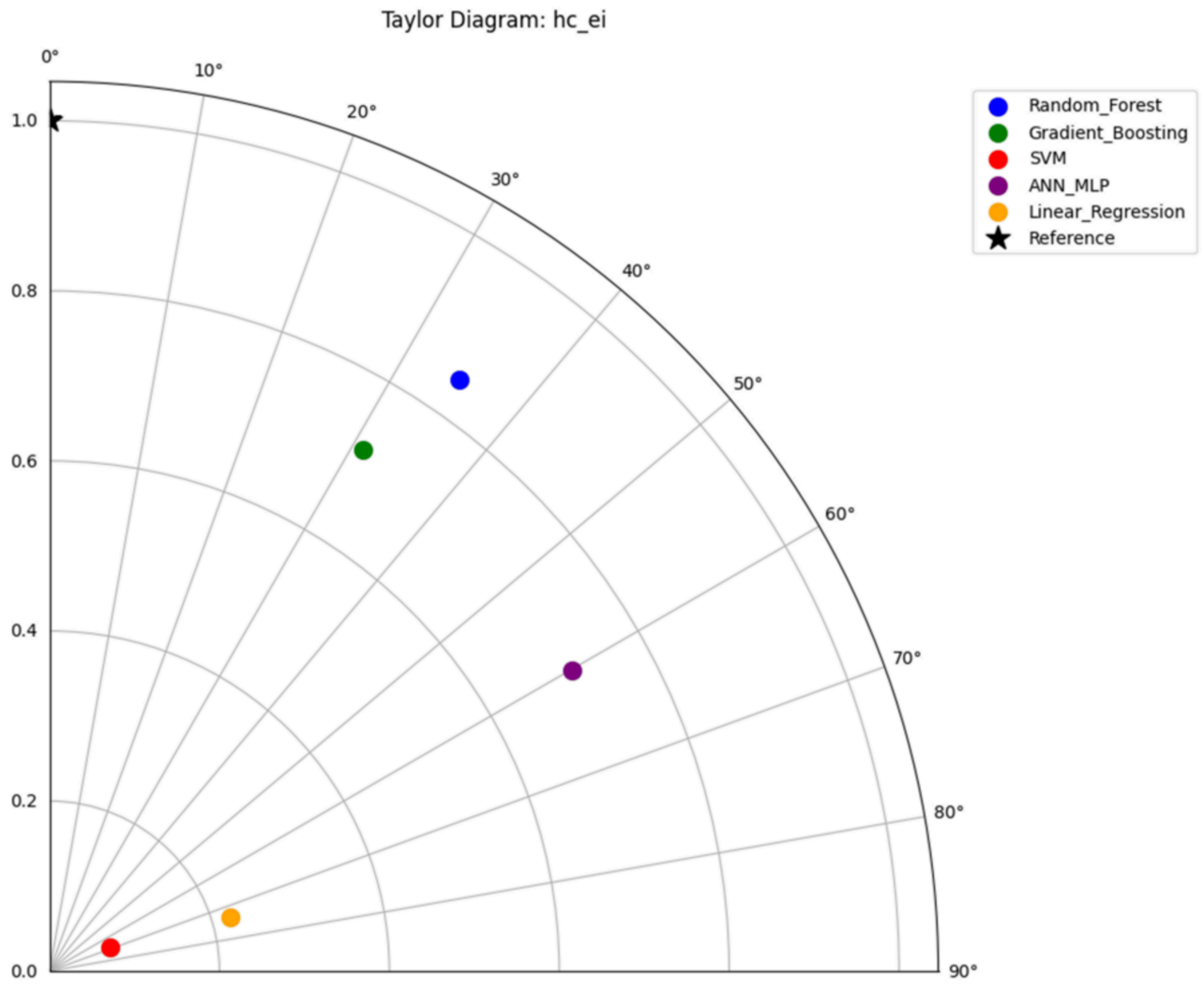


FIGURE 16: Taylor Diagram for HC Emission Index Prediction

ANN-MLP, Artificial Neural Network-Multi-Layer Perceptron; HC, Hydrocarbons; SVM, Support Vector Machine

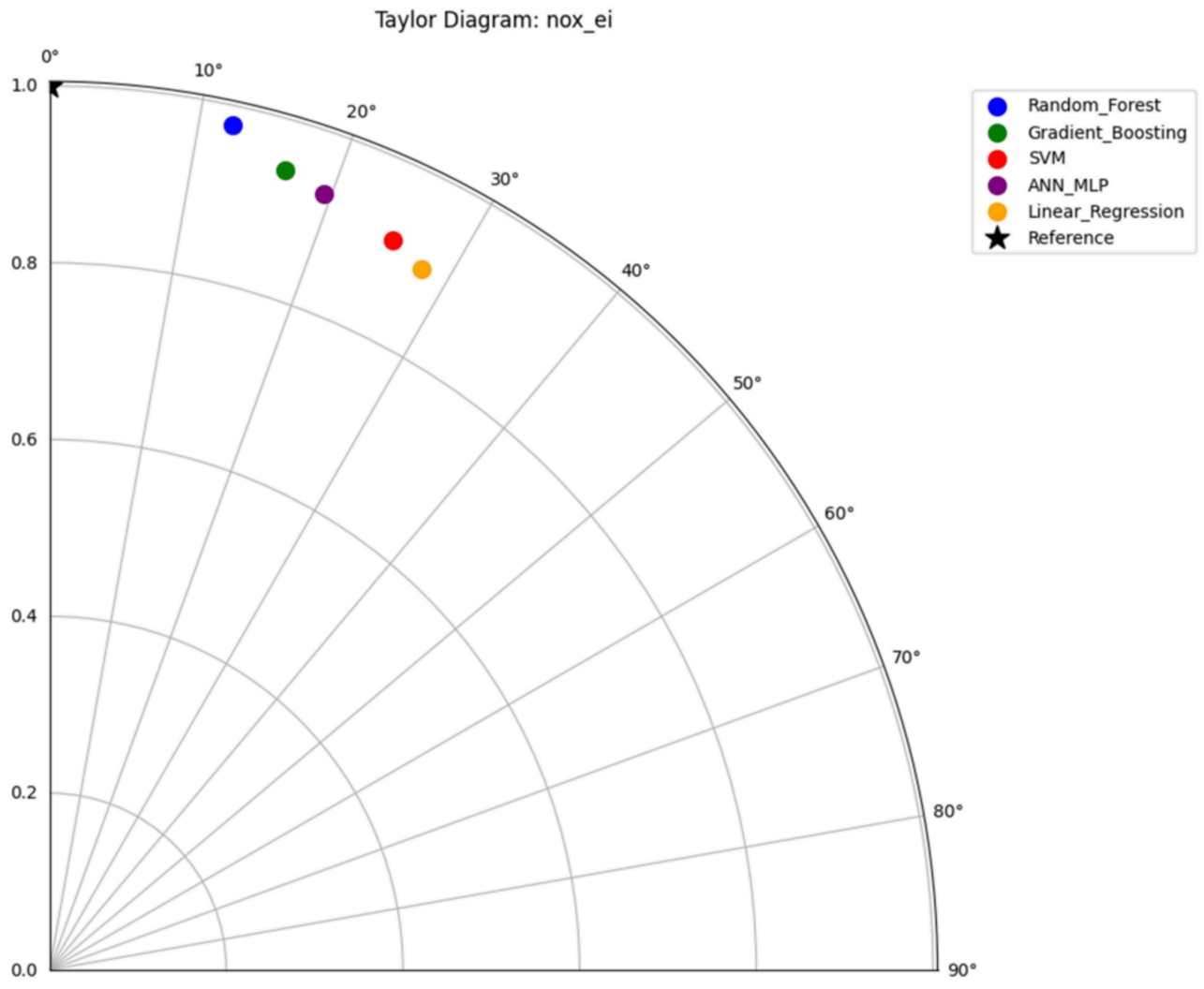


FIGURE 17: Taylor Diagram for NOx Emission Index Prediction

ANN-MLP, Artificial Neural Network-Multi-Layer Perceptron; SVM, Support Vector Machine

Conclusions

This study presented a data-driven ML framework for predicting aircraft engine emissions under the ICAO LTO cycle using certified ICAO emissions databank records. Multiple ML models were evaluated, with ensemble approaches demonstrating superior predictive capability. The Random Forest model achieved the best overall performance, yielding correlation coefficients of approximately 0.95 for NOx, 0.80 for CO, and 0.70 for HC, along with improved variance representation.

Feature importance analysis identified fuel flow as the dominant governing parameter across all emission species, while thrust and pressure ratio exhibited pollutant-specific secondary influences. Interpretability analyses confirmed physically consistent emission trends, revealing strong non-linear sensitivities for CO and HC at low-power regimes and monotonic NOx behaviour associated with high-temperature combustion conditions. Error variability assessment further highlighted phase-dependent prediction uncertainty, emphasizing the challenges of modeling incomplete combustion products during idle conditions and thermal NOx formation at high-power phases.

How to cite this article:
V S, PN S (March 10, 2026) Machine Learning–Based Prediction and Interpretability Analysis of Aircraft Engine Landing and Take-Off Emissions. Cureus J Comput Sci 3 : es44389-026-00038-6. DOI https://doi.org/10.7759/s44389-026-00038-6

Additional Information

Author Contributions

All authors have reviewed the final version to be published and agreed to be accountable for all aspects of the work.

Concept and design: Somashekar V, Shivakumar PN

Acquisition, analysis, or interpretation of data: Somashekar V, Shivakumar PN

Drafting of the manuscript: Somashekar V, Shivakumar PN

Critical review of the manuscript for important intellectual content: Somashekar V, Shivakumar PN

Supervision: Somashekar V

Disclosures

Human subjects: All authors have confirmed that this study did not involve human participants or tissue. **Animal subjects:** All authors have confirmed that this study did not involve animal subjects or tissue. **Conflicts of interest:** In compliance with the ICMJE uniform disclosure form, all authors declare the following: **Payment/services info:** All authors have declared that no financial support was received from any organization for the submitted work. **Financial relationships:** All authors have declared that they have no financial relationships at present or within the previous three years with any organizations that might have an interest in the submitted work. **Other relationships:** All authors have declared that there are no other relationships or activities that could appear to have influenced the submitted work.

Data Availability Statements

Data sharing is not applicable. This work is theoretical; no datasets were generated or analyzed.

References

1. Han B, Yao T, Li G, Song Y, Zhang Y, Dai Q, Yu J: Marginal reduction in surface NO2 attributable to airport shutdown: A machine learning regression-based approach. Environmental Research. 2022, 214:114117. 10.1016/j.envres.2022.114117
2. Bo X, Xue X, Xu J, Du X, Zhou B, Tang L: Aviation's emissions and contribution to the air quality in China. Atmospheric Environment. 2019, 201:121-131. 10.1016/j.atmosenv.2019.01.005
3. Wan J, Zhang H, Zhang Q, Li MZ, Xu Y: Deep learning framework for forecasting en route airspace emissions considering temporal-spatial correlation. Science of The Total Environment. 2023, 905:166986. 10.1016/j.scitotenv.2023.166986
4. Zhu C, Wu J, Liu M, Wang L, Li D, Kouvelas A: Recovery preparedness of global air transport influenced by COVID-19 pandemic: Policy intervention analysis. Transport Policy. 2021, 106:54-63. 10.1016/j.tranpol.2021.03.009
5. Rezo Z, Steiner S, Škurla Babić R: Comparative review of ICAO and EUROCONTROL flight carbon emission approximators. Sustainability. 2025, 17:6329. 10.3390/su17146329
6. Fichert F, Forsyth P, Niemeier HM: Aviation and Climate Change. Economic Perspectives on Greenhouse Gas Reduction Policies. Routledge, London; 2020. 10.4324/9781315572406
7. Mueller SC: Measuring and Modeling Aviation-Related Air Pollution in Near-Airport Communities. Boston University, Boston, MA; 2025.
8. Wen C, Lang J, Fu Y, et al.: Refined aircraft landing-takeoff activity modeling to improve the estimation of aviation CO2 and pollutants emissions. npj Climate and Atmospheric Science. 2025, 8:316. 10.1038/s41612-025-01195-6
9. Prashanth P, Eastham SD, Speth RL, Barrett SR: Aerosol formation pathways from aviation emissions. Environmental Research Communications. 2022, 4:021002. 10.1088/2515-7620/ac5229
10. Grobler C, Wolfe PJ, Dasadhikari K, et al.: Marginal climate and air quality costs of aviation emissions. Environmental Research Letters. 2019, 14:114031. 10.1088/1748-9326/ab4942
11. Eastham SD, Barrett SR: Aviation-attributable ozone as a driver for changes in mortality related to air quality and skin cancer. Atmospheric Environment. 2016, 144:17-23. 10.1016/j.atmosenv.2016.08.040

How to cite this article:
V S, PN S (March 10, 2026) Machine Learning–Based Prediction and Interpretability Analysis of Aircraft Engine Landing and Take-Off Emissions. Cureus J Comput Sci 3 : es44389-026-00038-6. DOI https://doi.org/10.7759/s44389-026-00038-6

12. Cameron MA, Jacobson MZ, Barrett SR, et al.: An intercomparative study of the effects of aircraft emissions on surface air quality. Journal of Geophysical Research: Atmospheres. 2017, 122:8325-8344. 10.1002/2016jd025594

13. Yim SH, Lee GL, Lee IH, et al.: Global, regional and local health impacts of civil aviation emissions. Environmental Research Letters. 2015, 10:034001. 10.1088/1748-9326/10/3/034001

14. Kalafatelis AS, Nomikos N, Giannopoulos A, Alexandridis G, Karditsa A, Trakadas P: Towards predictive maintenance in the maritime industry: A component-based overview. Journal of Marine Science and Engineering. 2025, 13:425. 10.3390/jmse13030425

15. Chati YS, Balakrishnan H: Statistical modeling of aircraft engine fuel flow rate. 30th Congress of the International Council of the Aeronautical Sciences, DCC, Daejeon, Korea. 2016, 1-10.

16. Kavallieratos G, Diamantopoulou V, Katsikas SK: Shipping 4.0: Security requirements for the cyber-enabled ship. IEEE Transactions on Industrial Informatics. 2020, 16:6617-6625. 10.1109/tii.2020.2976840

17. Gómez Ruiz MÁ, de Almeida IM, Pérez Fernández R: Application of machine learning techniques to the maritime industry. Journal of Marine Science and Engineering. 2023, 11:1820. 10.3390/jmse11091820

18. Angelopoulos A, Giannopoulos A, Nomikos N, Kalafatelis A, Hatziefremidis A, Trakadas P: Federated learning-aided prognostics in the shipping 4.0: Principles, workflow, and use cases. IEEE Access. 2024, 12:6437-6454. 10.1109/access.2024.3350777

19. Achouch M, Dimitrova M, Ziane K, Sattarpanah Karganroudi S, Dhouib R, Ibrahim H, Adda M: On predictive maintenance in industry 4.0: Overview, models, and challenges. Applied Sciences. 2022, 12:8081. 10.3390/app12168081

20. Kalafatelis AS, Trochoutsos C, Giannopoulos AE, Angelopoulos A, Trakadas P: A stacking ensemble learning model for waste prediction in offset printing. ICIEAEU '23: Proceedings of the 2023 10th International Conference on Industrial Engineering and Applications. 2023, 267-272. 10.1145/3587889.3588210

21. Zheng H, Paiva AR, Gurciullo CS: Advancing from predictive maintenance to intelligent maintenance with AI and IIOT. arXiv. 2020, 10.48550/arXiv.2009.00351

22. Dong Y, Tao J, Zhang Y, Lin W, Ai J: Deep learning in aircraft design, dynamics, and control: Review and prospects. IEEE Transactions on Aerospace and Electronic Systems. 2021, 57:2346-2368. 10.1109/taes.2021.3056086

23. Dong Y: Implementing Deep Learning for comprehensive aircraft icing and actuator/sensor fault detection/identification. Engineering Applications of Artificial Intelligence. 2019, 83:28-44. 10.1016/j.engappai.2019.04.010

24. Dong Y: An application of deep neural networks to the in-flight parameter identification for detection and characterization of aircraft icing. Aerospace Science and Technology. 2018, 77:34-49. 10.1016/j.ast.2018.02.026

25. Deepika J, Reddy PM, Murari K, Rahul B: Predictive maintenance of aircraft engines: machine learning approaches for remaining useful life estimation. 2025 6th International Conference on Mobile Computing and Sustainable Informatics (ICMCSI), Goathgaun, Nepal. 2025, 1679-1686. 10.1109/ICMCSI64620.2025.10883526

26. Gajghate SS, Noor MM, Kumar S, et al.: A transformer guided multi modal learning framework for predictive and causal assessment of thermal runaway in high energy batteries. Scientific Reports. 2025, 15:37054. 10.1038/s41598-025-20886-x

How to cite this article:
V S, PN S (March 10, 2026) Machine Learning–Based Prediction and Interpretability Analysis of Aircraft Engine Landing and Take-Off Emissions. Cureus J Comput Sci 3 : es44389-026-00038-6. DOI https://doi.org/10.7759/s44389-026-00038-6